Kevin Burgess
Texas A&M University, US

Biomedical

PET imaging PD1 expression

Some cancer cells evade destruction by the immune system by expressing checkpoint proteins. For instance, the checkpoint protein PD-1 can be recognised by the PD-L1 receptor on T-cells, suppressing signals to initiate destruction of the tumor tissue (Figure 1).

Humanised mAbs that disrupt the PD-1•PD-L1 protein-protein interaction are transforming some aspects of clinical oncology. However, there are patients for whom these mAbs are ineffective, perhaps because their tumors are using different checkpoint systems. Detection of which patients will respond to the mAbs currently can only be done via biopsy and analysis for levels of PD-1 expression, but this procedure cannot be performed for some tumours.

Gambhir and co-workers point out that if there were an imaging system that would reveal accumulation of PD-L1 expressing tumour infiltrating lympocytes (TILs) around the tumour that could be interpreted as a go-indicator for immunotherapy with anti-PD-1 mAbs (*Bioconj. Chem.*,doi: 5b00318).

Thus they conjugated such mAbs to the copper ligand DOTA, radiolabeled this with ^{64}Cu and were able to image TILs accumulating around PD-1 expressing tumors in mice.

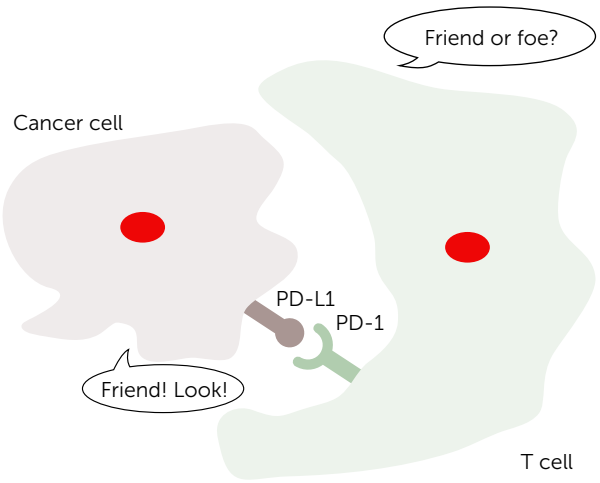

Figure 1 ***Some tumors 'play the PD-1 card' to evade destruction by the immune system***

PET Imaging of uPAR

Extravascular fibrin clearance is facilitated by uPA via the glycolipid-anchored, high-affinity receptor, uPAR. When uPAR interacts with uPA, the complex formed binds other extracellular proteins like vitronectin, integrins, G-protein-coupled receptors, low-density lipoprotein receptor-related protein 1 (LRP-1), and another protein called PAI-1. uPAR expression on normal cells is low or even undetectable. Thus the uPA•uPAR protein-protein interaction (Figure 2) appears to play pivotal roles in adhesion and tissue remodeling associated with metastasis.

A Danish group has been using a peptide 'AE105' that has high affinity for uPAR as a targeting module for positron emission tomography *in vivo*. In their latest contribution, they report labeling AE105 with (^{18}F-AlF)-NOTA complex facilitates imaging of prostate cancer *in vivo* (Kjaer *et al*, *Nuclear Med. Biol.*, 2015, **40**, 618).

Good radiochemical yields and images are obtained, although, curiously, this contribution does not attempt to assay metastatic spread.

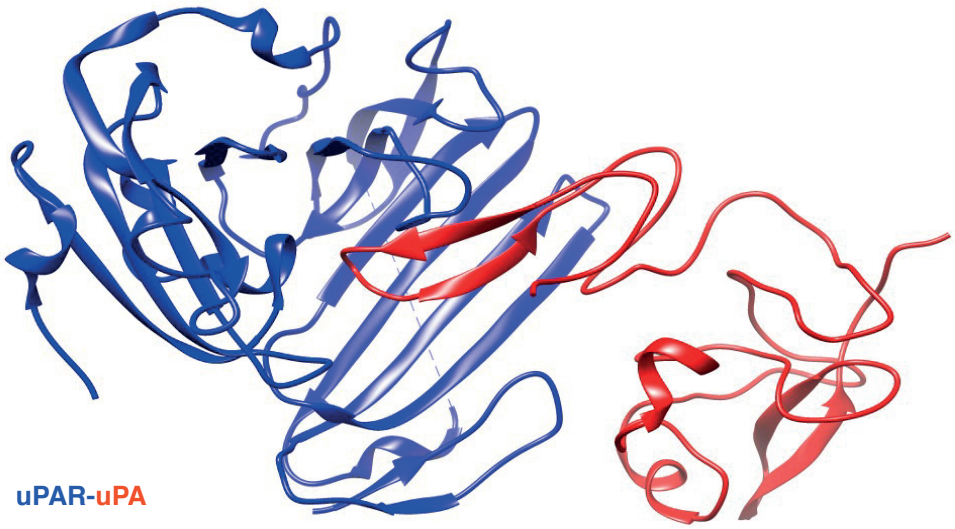

Figure 2 ***The uPA•uPAR protein-protein interaction activates proteolytic activity of uPA leading to tissue breakdown***

A method spawning methods

Bacteria use Clustered Regularly Spaced Palindromic Repeats (CRISPR sequences) after which they insert 'spacer DNA' derived from previous encounters with plasmids and phages to confer immunity against that type of DNA. This occurs when the spacer DNA binds its complement sequence in invading DNA, then via a series of steps recruits a nuclease called Cas9 to cleave the viral DNA.

In laboratory applications of CRISPR•Cas9 methodology, the RNA needed to recognise {any} strand of DNA is linked to the RNA necessary to recruit Cas9 by an RNA loop region. Thus, introduction of Cas9 and this RNA construct (single guide RNA, or sgRNA) can bring about cleavage of genomic DNA at any user-defined position. Ability to conveniently cleave genomic DNA makes it possible to knock out or knock in specific encoding sequences *in vitro* and *in vivo*.

A high level (*ie* quite hard to follow) mini-review of this technology was recently published (*Angew. Chem.*, 2015, **54**, 13508).

CRISPR•Cas9 methodology is a truly impactful advance because it can be adapted for so many different applications. For instance, Heald *et al* report *CRISPR•EATING* (Everything Available Turned Into New Guides), wherein ligation reactions can

be used to take genomic DNA and transform that into a series of sgRNA, notably avoiding the need to synthesise thousands of sgRNA fragments and enabling *live chromosome editing*.

Chemoselective Cys labeling in proteins, *in vitro* and in cells

In proteomics, iodoacetamide is the 'gold standard' reagent for labeling Cys residues, but that does not mean it is perfect. In fact, it has below optimal selectivity for the Cys thiol (relative to other nucleophilic sites in proteins, like Lys-amines), and it is less stable in aqueous media than desired.

Enter the group of Adibekian from Geneva, and Waser from Lausanne; their benziodoxolone reagent **1** only reacts with Cys residues in proteins (Figure 3), and it is more stable in aqueous media (*Angew. Chem. Int. Ed.*, 2015, **54**, 10852). Azide in this agent allows for tagging with biotin for pull down experiments, or fluorescent dyes.

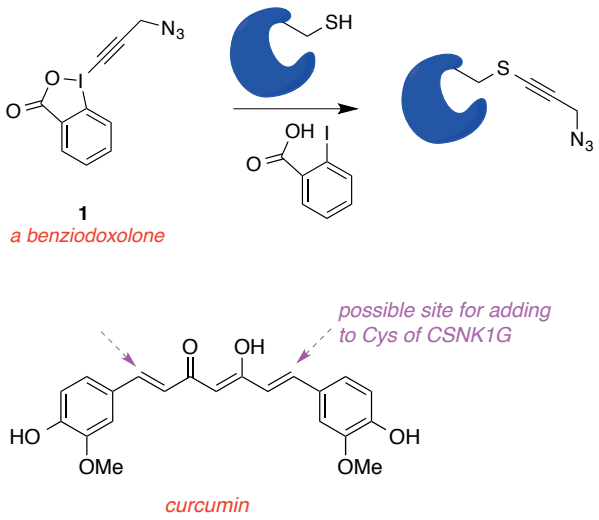

Figure 3 ***Reagent 1 is highly chemoselective for thiols in proteins; it has been used to identify a protein that may be alkylated by curcumin accounting for some beneficial properties of this natural product***

Thus it was shown that this system is stable in aqueous media, and could be used to label purified proteins, and total cell lysates. Comparative experiments showed while iodoacetamide and **1** labeled the same 1391 peptides, another 866 (38 %) were *only* labeled by **1**.

Moreover, further analyses showed that 97 % of the proteins labeled using **1** were tagged on Cys, compared with 91.4 % by iodoacetamide, *ie* the latter gives more false positive results.

Finally, the authors hypothesise that the mode of action of curcumin might be as a Michael acceptor electrophile for Cys residues. Thus they compared the tagged proteome for cells treated and not treated with curcumin. Curcumin blocked labeling of 57 proteins and one of these, casein kinase I gamma, is known to impact Akt signaling when inhibited, just as curcumin does, implying this is a likely target of the natural product.

Nigel P Freestone
University of Northampton, UK

Applied highlights

Stencilled self-propulsion engines

Millimetre-sized motors shaped like fish, swim autonomously while performing specific functions, eg water purification, can now be produced on an enormous scale by 2D screen-printing fabrication (R. Kumar, M. Kiristi, F. Soto, J. Li, V. V. Singha, J, Wang; *RSC Adv.*, 2015, **5**, 78986) (*C&I*, 2015, **10**, 6).

Nano- and micro-sized machines that convert chemical reactions into motion have been on the drawing board for many years; however, they are complicated and expensive to make through electrodeposition, sputtering and lithography fabrication techniques.

The new screen-printing approach offers large-scale cost-effective fabrication of efficient multi-functional chemically-powered motors. Diverse fish architectures, consisting of several predesigned printed layers, including the mid-body, head, tail, and an entire fish, are achieved by printing different functional inks through the corresponding patterned stencils.

The 2D fish-printing approach allows fine control of the shape, size, functionality and performance of the resulting fish swimmers. In particular, different functionalities can be incorporated at specific areas by sequential printing of specific layers based on different modified inks. For example, printing of catalytic tails containing various Pt loadings has been used to prepare fish with different propulsion efficiencies. Inks based on activated carbon powder have been used for accelerated removal of chemical pollutants. Nickel-containing carbon ink has been used for magnetic control of the fish directionality.

This screen-printing fabrication route can be readily extended for incorporating other functional materials into one swimmer structure. Such a versatile, simple, scalable, fast, and cost-effective approach holds considerable promise for creating biomimetic swimmers with different properties for diverse practical applications.

Self-folding graphene paper

A graphene-based paper has been developed that can fold itself into predesigned shapes when exposed to light or gentle heat (J. Mu, C. Hou, H. Wang, Y. Li, Q. Zhang, M. Zhu; *Science Advances*, doi: 10.1126/sciadv.1500533) (*C&I*, 2015, **12**, 18).

Created from graphene oxide, the material can also 'walk' across a table and turn a corner. Potential

applications of the material include sensors, artificial muscles, robotics and even smart clothes, which could change shape and style in response to body temperature, environmental changes, or other gentle simulations.

To produce the mechanical folding effect, graphene oxide-polydopamine (GO-PDA) layers are deposited in a pattern onto a graphene oxide base. The GO-PDA layers contain water absorbed from the environment. Shining infra-red or laser light onto the paper led to the water evaporating and causing the layers to shrink, bending the paper into the designed shape. When the light is extinguished the GO-PDA quickly reabsorbs water and the paper unfolds.

The researchers have produced a hand shaped device can to grip and release objects, and strips of the material can mimic the locomotion of a caterpillar when the light is repeatedly flashed on and off.

Antimony from lamp phosphor waste

The European Commission recently identified antimony as one of the most critical elements with a supply risk; at present, 90% of world production is in China. With mines in Europe unlikely to reopen, a secondary production source is needed to satisfy demand.

Belgium researchers have developed a method to extract antimony from lamp phosphor waste {(Ca,Sr)5(PO4)3(Cl,F):Sb3+,Mn2+ (HALO)} and convert residues from the process into fertiliser (D. Duponta, K. Binnemans; *Green Chem.*, doi: 10.1039/C5GC01746G).

This approach is completely non-toxic with the only by-product being sodium chloride – table salt – which is easily discarded. The HALO phosphor is first dissolved in HCl, followed by a selective extraction of antimony with the ionic liquid *Aliquat 336*. The remaining aqueous solution is treated with sodium hydroxide, which precipitates calcium phosphate – a useful material for fertilisers and other applications.

This process can be integrated in lamp phosphor recycling schemes aimed at recovering the rare earths from HALO.

Solar energy collector

Scientists in the US have for the first time made a solar energy collector using carbon nanotubes that can directly convert optical light in to a direct current (A. Sharma, V. Singh, T. L. Bougher, B. A. Cola; *Nature Nanotechnology*, doi:10.1038/nnano.2015.220).

It is hoped these optical rectennas may one day rival established technologies, such as the silicon solar cell; optical rectennas were first proposed over 40 years ago.

Antennae collect electromagnetic radiation, convert the signal into an alternating current, much like a radio antenna, before sending the current through a diode, which converts it to a direct current.

Due to fabrication challenges at the nanoscale, this concept has not been demonstrated experimentally, until now. Rather than construct a rectenna with two discrete components that act as either an antenna or diode, the researchers used carbon nanotubes that can be both simultaneously.

This was achieved by growing 10μm high vertical array of billions of carbon nanotubes on a silicon substrate via chemical vapour deposition. Each nanotube is coated with an aluminium oxide insulator and capped with an aluminium anode.

The metal–insulator–metal sandwich structure allows the nanotube array to behave as both a light harvester and a tunnel diode. Electrons excited within the nanotube by light absorption tunnel through the insulator to the metal anode and the current flow is converted into DC. Power rectification is observed under simulated solar illumination, and there is no detectable change in diode performance after numerous current–voltage scans between 5 and 77°C, indicating a potential for robust operation.

Calcium carbide replaces explosive acetylene in organic synthesis

Vinyl thioesters, important building blocks for synthesising sulfur-functionalised polymers, are usually synthesised from acetylene using complicated high-pressure equipment under highly basic hazardous conditions and at high cost. Scientists from the Russian Academy of Sciences have developed a safer, greener and cheaper process using widely available and stable calcium carbide as the starting material (K. S. Rodygin and V. P. Ananikov, *Green Chem.*, doi 10.1039/c5gc01552a) (Scheme 1).

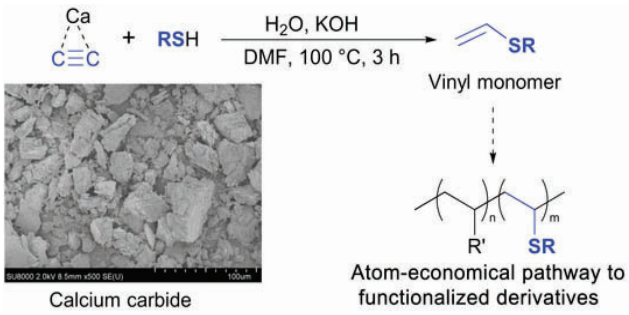

Scheme 1

Calcium carbide reacts with a carefully dosed amount of water to generate acetylene directly inside a flask resulting in the formation of vinyl thioesters. The reaction proceeds under mild conditions using a standard laboratory setup and can be been scaled up to synthesise grams of sulfides with the potential to scale up further.

Hollow metal–organic nanoparticles

Hollow metal–organic nanoparticles (MOPs) are now available through the simple addition of metal ions into solutions of organic boronate nanoparticles (BNP), produced from the simple condensation-driven cooperative polymerisation of a bisimido boronic acid (Im-BA) molecule and a bisimido catechol (Im-Ca) molecule in methanol. MOP shell thickness can be easily

Scheme 2

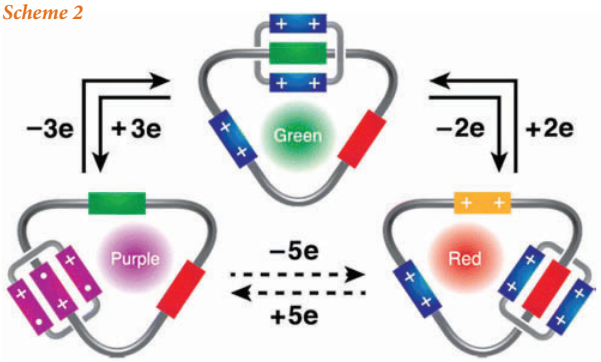

tuned by the concentration of metal ions in solution (L. Li, C. Yuan, D. Zhou, A. E. Ribbe, K. R. Kittilstved, S. Thayumanavan; *Angew. Chem. Int. Ed. Engl.*, 2015, **54**, 12991). These hollow nanoparticles have numerous applications, such as catalysis, sensing, storage, and biomedicine.

Electrochromic tristable molecular switch

A tristable [2]catenane, composed of a macrocyclic polyether incorporating 1,5-dioxynaphthalene (DNP) and tetrathiafulvalene (TTF) units along with a 4,4′-bipyridinium (BIPY•+) radical cation as three very different potential recognition sites, interlocked mechanically with the tetracationic cyclophane; cyclobis(paraquat-p-phenylene) (CBPQT4+), was synthesised by donor–acceptor templation, employing a 'threading-followed-by-cyclization' approach (J. Sun, Y. Wu, Y. Wang, Z. Liu, C. Cheng, K. J. Hartlieb, M. R. Wasielewski, J. F. Stoddart; *J. Amer. Chem. Soc.*, 2015, **137**, 13484) (Scheme 2).

In this catenane, movement of the CBPQT4+ ring in its different redox states among these three potential recognition sites, with corresponding color changes, is achieved by tuning external redox potentials.

In the starting state, where no external potential is applied, the ring encircles the TTF unit and displays a green colour. Upon oxidation of the TTF unit, the CBPQT4+ ring moves to the DNP unit, producing a red colour. Finally, if all the BIPY2+ units are reduced to BIPY•+ radical cations, the resulting CBPQT2(•+) diradical dication will migrate to the BIPY•+ unit, resulting in a purple colour.

These readily switchable electrochromic properties render the [2]catenane attractive for use in electro-optical devices.

Silica aerogels

Silica aerogels are attractive candidates for thermal, catalytic, pharmaceutical and chemical applications because of their exceptional physical properties, such as low density (0.1gcm^3) and thermal conductivity (12–15mWm^{-1}K^{-1}) and high porosity (>95 %) and specific surface areas (800–1000m^{2}g^{-1}).

However, the widespread use of silica aerogels has been prevented by their poor mechanical properties and concerns about dust release.

Silica aerogels are inherently fragile because of the weak pearl-necklace-like structure: the three-dimensional network consists of silica nanoparticles with diameters of 3–10nm connected by narrow inter-particle necks.

Mechanically stable and superinsulating nanoscale interpenetrating pectin–silica hybrid aerogels can be obtained by dissolving pectin with a high methoxy (HM) content directly into an aqueous, water-glass-derived silicic acid solution, followed by cogelation, solvent exchange, hydrophobisation, and drying with supercritical CO2 (S. Zhao, W. J. Malfait, A. Demilecamps, Y. Zhang, S. Brunner, L. Huber, P. Tingaut, A. Rigacci, T. Budtova, M. M. Koebel; *Angew. Chem. Int. Ed. Engl.*, 2015, **54**, 14282).

Their structural and physical properties can be tuned by adjusting the gelation pH and pectin concentration. Hybrid aerogels made at pH1.5 exhibit minimal dust release and vastly improved mechanical properties while remaining excellent thermal insulators. The change in the mechanical properties is directly linked to the observed "neck-free" nanoscale network structure with thicker struts. Such a design is superior to 'neck-limited', classical inorganic aerogels.

This new class of materials opens up new perspectives for novel silica–biopolymer nanocomposite aerogels.

Nanofluidic diodes

A smart nanofluidic diode that exhibits both ion gating and ion current rectification has been developed using a1-(4-amino-phenyl)-2,2,2-trifluoro-ethanone-functionalised, conical nanochannel in a polyimide (PI) membrane (Ganhua Xie, Kai Xiao, Zhen Zhang, Xiang-Yu Kong, Qian Liu, Pei Li, Liping Wen and Lei Jiang; *Angew. Chem. Int. Ed. Engl.*, 2015, **54**, 13664).

The switch-like property can be tuned by controlling the wettability and charge distribution with carbonate ions. Such a nanodevice is advantageous for precisely controlling conductive states with an ultrahigh gating ratio of up to 5000, and a high rectification ratio of 27.

By virtue of the high selectivity and sensitivity for carbonate ions, this nanofluidic diode may find applications in carbonate or carbon dioxide detection.

G. Richard Stephenson
University of East Anglia, UK

Organic chemistry

Homing in on holes

The removal of an electron from a cyclic p-polyphenylene to form a radical cation (*eg* **1**) introduces a 'hole' but surprising effects have been identified with larger ring-sizes (Figure 1). The 'hole distribution' was assessed by calculating the properties of the highest occupied molecular orbital (HOMO), which for the π system of a radical cation will contain a single electron. This is evenly distributed for small rings such as n = 5 or 6, but for larger rings the HOMO, and consequently the hole distribution, is restricted to just seven of the rings. In this respect, linear and cyclic polyphenylenes have similar properties, but the trends in the variation of oxidation potentials with ring-size/chain-length is very different (M. R. Talipov, R. Jasti, R. Rathore; *J. Am. Chem. Soc.*, 2015, **137**, 14999).

Three-way sorting

Molecular cages with different shapes and dimensions can be formed by using suitable organic links (Figure 2) between metal ions (Fe^{II} in this case). Two tetrahedral cages (one

large and one small) and a cubic cage have now been sorted between three immiscible phases, formed by floating a water layer on top of a [P6,6,6,14][NTf_2] layer, which itself floats on an [emim][NTf_2] layer (A. B. Grommet, J. L. Bolliger, C. Browne, J. R. Nitschke; *Angew. Chem. Int. Ed.*, 2015, **54**, 15100).

The small tetrahedron, formed using linker **2**, remains in the water; the cube, formed using linker **3**, occupies the trihexy(tetradecyl) phophonium **8** ([P6,6,6,14]$^+$) layer; and the large tetrahedron, formed using linker **4**, occupies the 1-ethyl-3-methylimidazolium **9** ([emin]$^+$) layer. Equally intriguingly, three small molecules (**5**-**7**), which form selective inclusion complexes within the cages, were also sorted in this way.

Coiling up in a cage

Miscible mixed-solvents systems can also influence the inclusion complexation properties. An example has been reported using deep cavitands that can form dimeric cages (J. V. Gavette, I. D. Petsalakis, G. Theodorakopoulos, K.-D. Zhang, Y. Yuc, J. Rebek Jr., *Chem. Commun.*, 2015, **51**, 17604).

Mixing 1,1,1,3,3,3-hexafluoro-isopropanol (HFIP) and water to accelerate the dissolution of **12**, also influences the conformational equilibrium to favour the deep pocket form, which itself can accommodate n-hydrocarbons as guest molecules.

Octane tends to occupy a single cavity but heptane is long enough to be shared between the two halves of the dimer **13** (Figure 3). Even longer alkanes can coil round inside the cavity allowing the rims of the two halves of the cage to remain in close contact.

Figure 1 ***Radical cations formed by oxidation of cyclic and linear p-polyphenylenes containing n para-linked benzene rings***

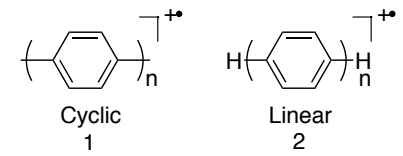

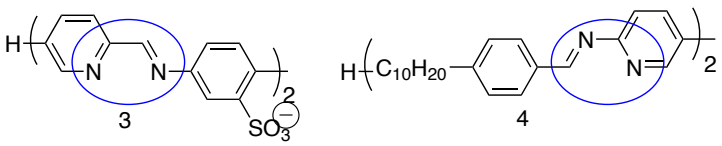

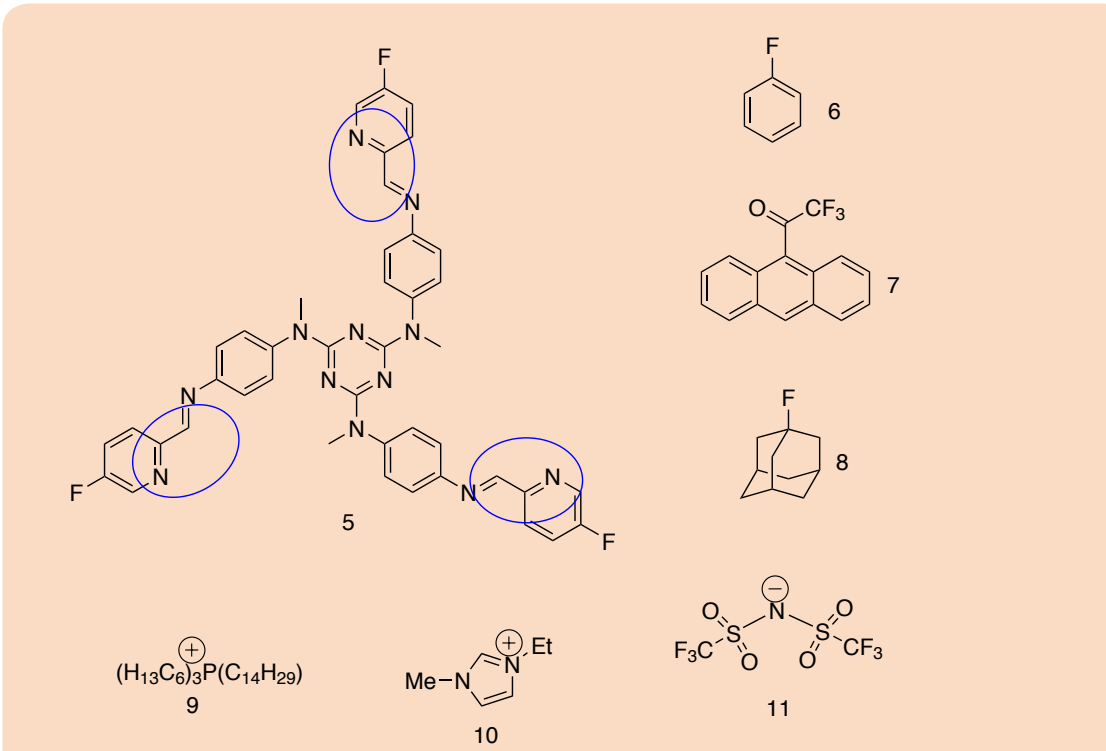

Figure 2, above right, ***Three edge- (3 and 4) or face-forming (5) ligands (the FeII-binding positions are ringed) and three small guest molecules [fluorobenzene (6), 9-trifluoromethylacetylanthracene (7) and 1-fluoroadamantane (8)]; the ionic liquids formed from cations 9 and 10 and their counterion (TfO)2N– (11) are illustrated in the box***

Figure 3, right, ***Part-structure A illustrates one of the four corners of the deep-pocket cavitand 12; for the structure of 1,1,1,3,3,3-hexafluoroisopropanol (HFIP), see box***